OVERVIEW OF THE URBAN WIRELESS LOCALIZATION COMPETITION

Çağkan Yapar[†] *Fabian Jaensch*[†] *Ron Levie*[‡] *Gitta Kutyniok*[*§¶] *Giuseppe Caire*[†]

[†]Technical University of Berlin, [‡]Technion – Israel Institute of Technology
[*]Ludwig Maximilian University of Munich, [§]University of Tromsø
[¶]Munich Center for Machine Learning (MCML)

ABSTRACT

In dense urban environments, Global Navigation Satellite Systems do not provide good accuracy due to the low probability of line-of-sight (LOS) between the user equipment (UE) to be located and the satellites due to the presence of obstacles such as buildings. As a result, it is necessary to resort to other technologies that can operate reliably under non-line-of-sight (NLOS) conditions. To promote research in the reviving field of radio map-based wireless localization, we have launched the *MLSP 2023 Urban Wireless Localization Competition.* In this short overview paper, we describe the urban wireless localization problem, the provided datasets and baseline methods, the challenge task, and the challenge evaluation methodology. Finally, we present the results of the challenge.

***Index Terms*—** challenge, deep learning, radio map, received signal strength (RSS), time of arrival (ToA), wireless localization.

1. INTRODUCTION

Localization of a User Equipment (UE), has many important applications such as in autonomous driving [1], proof of witness presence [2],5G networks [3], emergency 911 services [4], or intelligent transportation systems [5].

In dense urban environments, line-of-sight links between the UE to be located and the satellites are very often non-existent, which greatly degrades the positioning accuracy of Global Navigation Satellite Systems (GNSS) [6]. In addition, handheld devices suffer from very high battery consumption to detect the low power satellite signals. Therefore, other technologies should be used for reliable positioning in urban environments. Due to their ubiquity, cellular and WiFi networks are considered as strong candidates, where the measured characteristics of the beacon signals from multiple transmitters (Tx) of the wireless system are used for localization, e.g. Time of Arrival (ToA) [7], Time Difference of Arrival (TDoA), Angle of Arrival (AoA) and Received Signal Strength (RSS) [8].

1.1. Ranging vs Fingerprint (Radio Map)-Based Methods

In environments with many obstacles, distance estimates based on signal characteristics such as RSS, ToA, or other forms of channel state information are considered to be inaccurate, and thus methods for high accuracy should not rely on such intermediate distance (range) estimates.

The alternative is to avoid such inappropriate modeling assumptions and directly use the databases of radio signal signatures assigned to locations in the environment map. These so-called fingerprint-based methods match RSS or other channel state information with known measurements from a database and estimate the location based on similarity. Standard approaches include k-nearest neighbors (kNN) [9].

1.2. Measurement Campaigns vs Propagation Prediction

Fingerprinting traditionally refers to obtaining such radio signature databases (*radio maps*) through measurement campaigns. However, measurement campaigns are very labor-intensive and expensive endeavors. Moreover, the dense sampling required for high-precision localization is simply not feasible. Therefore, the use of deterministic simulations based on accurate propagation models such as ray tracing (which is based on high-frequency approximation of Maxwell's equations) is considered to be a more feasible and accurate approach than measurement campaigns to build the fingerprint databases. The drawback of such conventional accurate computational propagation prediction methods is their high computational complexity, which makes them unsuitable for real-time applications, such as the current task of interest, the wireless localization problem. Recently, many researchers, including the authors [10] of the current paper, have presented deep learning-based pathloss map estimation algorithms, which can estimate pathloss radio maps with high accuracy, but much faster than a conventional high-precision simulation. Based on this new possibility of accurate and fast pathloss radio map estimation, we have revisited the RSS fingerprint-based localization problem in [11, 12, 13, 14].

979-8-3503-2411-2/23/$31.00

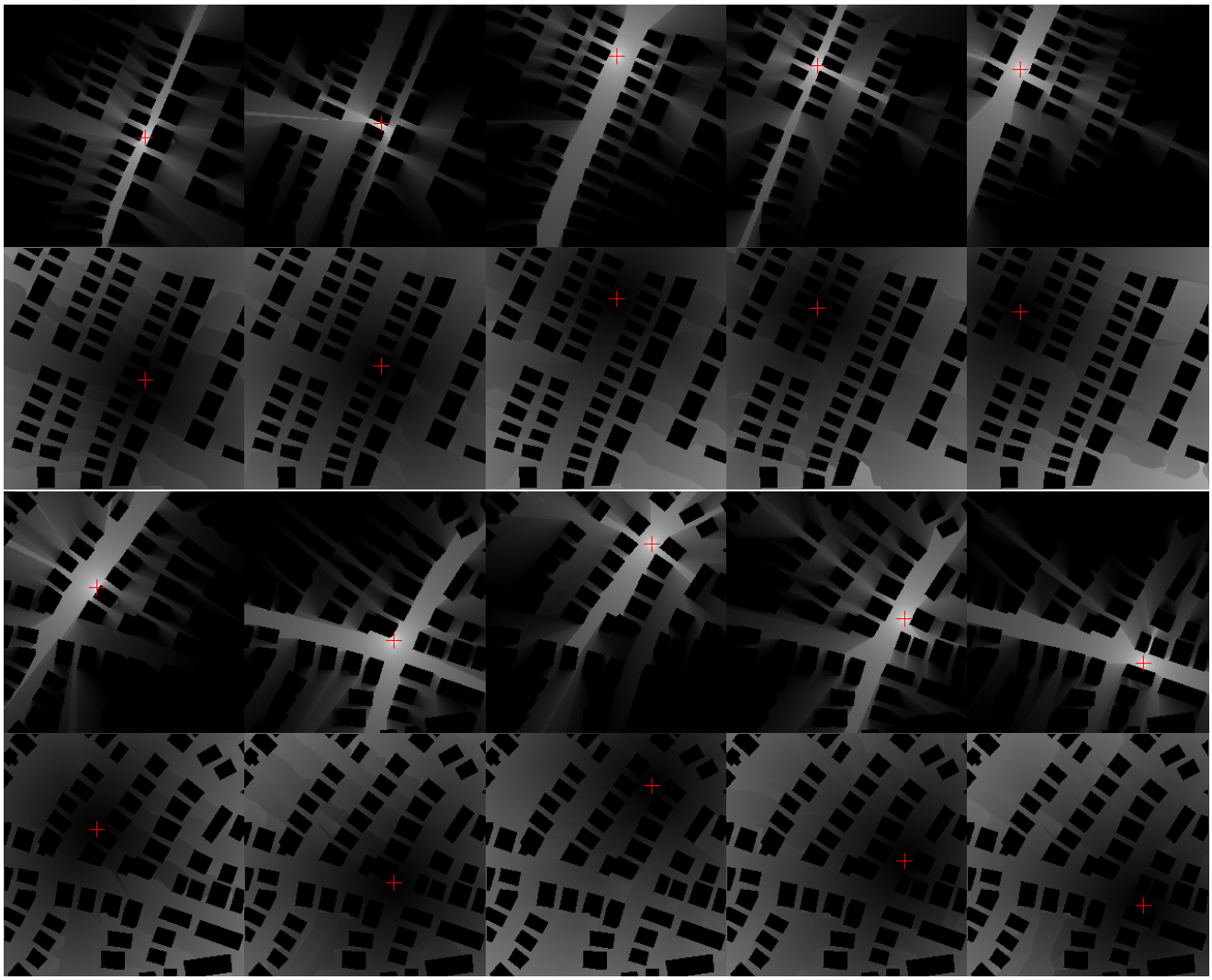

Fig. 1: Examples of pathloss and ToA radio maps from *RadioLocSeer* and *RadioToASeer* datasets. 5 simulated radio maps with different Tx positions for two city maps are shown. Tx positions are marked with a red plus sign. **Rows 1, 3:** Pathloss radio maps. **Rows 2, 4:** Corresponding ToA radio maps.

2. DATASETS

2.1. Training Datasets

The localization radio map datasets that we provided for the competition, namely the *RadioLocSeer* and the *RadioToASeer* datasets were first presented in our recent paper about our deep learning and pathloss-based localization method *LocUNet* [13], and are available at [15]. More details about them can be found in [16].

These datasets feature 99 different urban city maps of size $256m \times 256m$, which were fetched from OpenStreetMap [17] from the city maps of Ankara, Berlin, Glasgow, Ljubljana, London, and Tel Aviv. On each of these city maps, 80 different street level (1.5m) Tx locations were considered, with their positions being restricted to lie inside the central square of size 150m×150m, separated by at least 20 m from each other. The wireless propagation software Winprop from Altair [18] was used for the simulations for a dense grid of size $1m^2$ at the same height of 1.5m, amounting to a total of 7920 radio map simulations, and under various simulation models.

2.1.1. RadioLocSeer Dataset

The dataset contains pathloss radio map simulations based on the *Intelligent Ray Tracing (IRT)* [19] and the Dominant Path Model (DPM). High accuracy of these method were proven by field measurements in several cities, see e.g. [20], [21] or [22] and the references therein.

In this competition, we focused only on one type of simulation, DPM, for simplicity, which we describe in Sec. 2.1.3 shortly. See our previous work [13, 12] for the consideration of different simulation models/radio map estimation methods and environment maps to emulate the potential mismatch of radio map estimation and real life measurements.

The results of the pathloss simulations are provided as 8-bit `.png` image files, which were obtained by post-

processing of the simulation results by first converting the pathloss values P_L to pixel values between 0 and 1 by $p = \max\{\frac{P_L - P_{L,thr}}{P_{L,max} - P_{L,thr}}, 0\}$, where $P_{L,max}$=-47 dB denotes the maximal pathloss in all radio maps in the dataset and $P_{L,thr}$=-127 dB is the pathloss threshold, below which the RSS is assumed to be not large enough for successful detection [10, 16].

2.1.2. *RadioToASeer Dataset*

This dataset contains the ToA radio map counterparts of the *RadioTLocSeer Dataset*, i.e. the ToA of the dominant paths (in ns), to allow for comparisons between RSS and ToA ranging-based methods in realistic urban scenarios. This dataset is provided in `.mat` format. The file can be directly read, or if necessary after conversion to the desired file format. Similar to the procedure applied to the pathloss simulations, ToA radio maps in `.png` format can also be generated.

In Fig. 1 we show examples of two city maps and pathloss and ToA radio maps of 5 Tx different Tx deployments. Here, to obtain ToA radio maps as 8-bit `.png` images, we first employed the scaling of simulated ToA values T, to pixel values between 0 and 1 by $t = \frac{T}{T_{max}}$, where T_{max} denotes the maximum ToA in all the dataset.

Note that due to the property of dominant paths being the shortest free space path, we argued in [13, 16] that evaluating ToA-based localization algorithms using *RadioToASeer* yields (quasi-)upper bounds for their performances in real deployment.

2.1.3. *Dominant Path Model (DPM) [21]*

DPM is based on the assumption that the dominant (i.e. the one subject to least attenuation) propagation path from Tx to UE must arrive via convex corners of the obstacles to UE, and thus only diffractions are taken into account, which is equivalent to finding the shortest free space path to each point.

The pathloss values are then calculated based on the specifications (e.g. the length of the path, angles of diffractions) of the found dominant path for each point on the grid.

2.2. Test Dataset

For the fair evaluation of the participants' methods, we prepared a test dataset which was not published before. 84 city maps of size 256×256 were obtained from *OpenStreetMap* [17] in Istanbul, and again 80 different Tx positions per map were considered, amounting to 6720 pathloss and ToA simulations. The same simulation parameters were used as for *RadioLocSeer* and *RadioToASeer*. We dubbed this new test dataset *LocRSSToATest*, as it is a bundle of both pathloss and ToA radio maps. An example pathloss and the associated ToA radio maps from the dataset are shown in Fig. 2.

3. THE COMPETITION TASK

The task of the challenge was to estimate the location of UE by using either or both the RSS and the ToA measurements

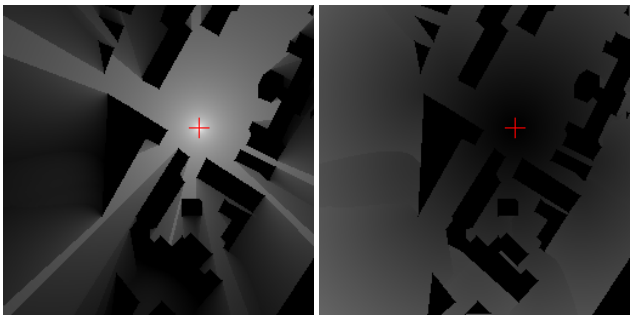

(a) Pathloss radio map (b) ToA radio map

Fig. 2: An example pathloss and the corresponding ToA radio map from *LocRSSToATest Dataset*. Tx positions are marked with a red plus sign.

from several anchor (i.e. stationary) Tx and estimations of pathloss and ToA radio maps for each such Tx. Notice that assuming constant transmit power, the RSS radio map estimations can be obtained from pathloss radio maps through the relation (in dB scale), $P_{UE} = P_L + P_{Tx}$, where P_{Tx} and P_{UE} denote the transmit power and the RSS, respectively.

The accuracy of the radio map estimates depends on the availability of detailed and reliable knowledge of the propagation environment, i.e. the shape and material of the objects (such as buildings or vegetation) in the propagation environment. Even if such information is available, the presence of moving objects in the environment, such as cars and pedestrians, leads to an inevitable discrepancy between the estimates and the real measurements. Therefore, participants were asked to develop methods that are robust to realistic inaccuracies in their radio map estimates. For simplicity, we proposed to model the mismatch between the available and real RSS and ToA information by additive Gaussian noise terms, see also [23, 14, 13].

4. EVALUATION METHODOLOGY

The accuracy of the submitted methods were evaluated by the root mean square error (RMSE), between the estimated and the true UE locations, given by

$$\text{RMSE} = \sqrt{\frac{1}{|\mathcal{T}|}\sum_{k\in\mathcal{T}} ||\mathbf{u}^k - \tilde{\mathbf{u}^k}||_2^2},$$

where $\tilde{\mathbf{u}^k} := (\tilde{x}^k, \tilde{y}^k)$ and $\mathbf{u}^k := (x^k, y^k)$ denote the location estimate and the true location of the kth instance of a test dataset $\mathcal{T}$.

5. BASELINE METHODS

5.1. Probabilistic Formulation of the Localization Problem

In the following, we provide a simple yet very important formulation of the localization problem [14], which provides

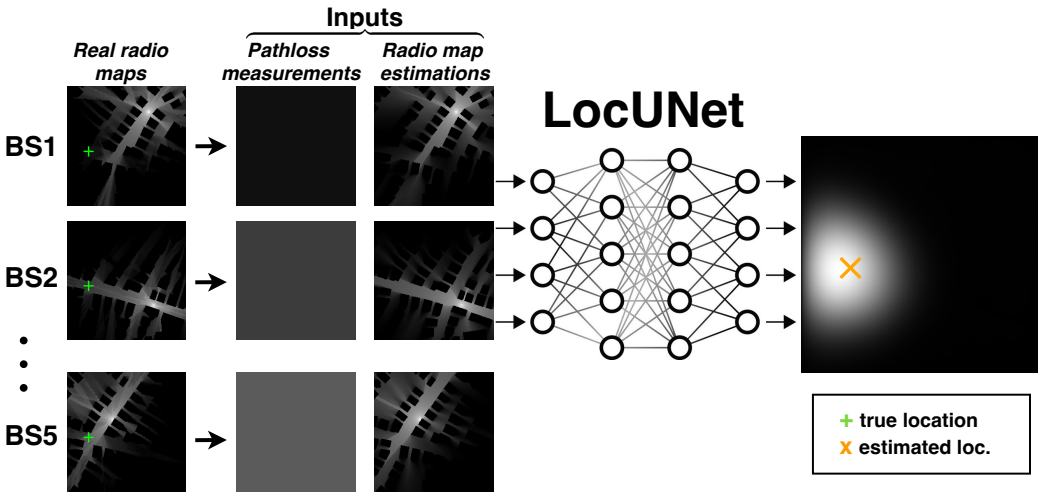

Fig. 3: A visual summary of the baseline method - LocUNet [13]- with 5 anchor Txs. The UE located at the coordinate indicated with green plus sign measures the true RSS values from each Tx (base station/BS). Together with the radio map estimates, the measured values (represented with images of the same size as radio map estimates, with each pixel having the value of the measurement) constitute the inputs of the LocUNet. The location estimate (orange cross) is found by taking the center of mass of the heatmap indicated in gray level.

performance upper bounds under specific settings, and hence can serve as an ultimate benchmark for localization methods. For ease of exposition, we consider localization based only on one type of radio signal signature (e.g. RSS or ToA), but the formulation straightforwardly translates into multi-signature settings.

Let us consider a finite set $\mathbb{D}$ of possible UE locations in the two-dimensional plane. The localization task is then to estimate the position $y_0 \in \mathbb{D}$ of an UE measuring a wireless signal signature $\mathbf{r} = (r_1, \ldots, r_N) \in \mathbb{R}^N_{\geq 0}$ obtained from N anchor transmitters $\mathrm{Tx}_1, \ldots, \mathrm{Tx}_N$, which can be formulated as a minimum mean square error (MMSE) problem ,

$$\hat{y}_0(\mathbf{r}) = \mathrm{argmin}_{f \in L^2(\mathbb{R}^N_{\geq 0}, \mathbb{D})} \mathbb{E}\left[\|y_0 - f(\mathbf{r})\|_2^2\right], \qquad (1)$$

which is solved by the posterior mean estimator (PME)

$$\hat{y}_0(\mathbf{r}) = \mathbb{E}\left[y_0 \,|\, \mathbf{r}\right] = \sum_{y_0 \in \mathbb{D}} y_0 \, p(y_0 \,|\, \mathbf{r}), \qquad (2)$$

where, with the usual abuse of notation, p denotes the probability density functions (pdf) of different variables. If the prior distribution of the location y_0 and the distribution of the true signal signature conditioned on the location $p(\mathbf{r} \,|\, y_0)$ are known, the PME can be calculated using Bayes' theorem,

$$\hat{y}_0(\mathbf{r}) = \sum_{y_0 \in \mathbb{D}} y_0 \, \frac{p(\mathbf{r} \,|\, y_0)\, p(y_0)}{\sum_{y \in \mathbb{D}} p(\mathbf{r} \,|\, y)\, p(y)}. \qquad (3)$$

In our localization setting based on radio maps (fingerprints), we have the estimated (previously stored) signal signature values $\mathbf{c}(y) = (c_1(y), \ldots, c_N(y)) \in \mathbb{R}^N_{\geq 0}$ available for each location $y \in \mathbb{D}$ and all N Tx. The true radio signature $\mathbf{r} \in \mathbb{R}^N_{\geq 0}$ measured by the UE is assumed to show a certain mismatch $\mathbf{z} = (z_1, \ldots, z_N) = \mathbf{r} - \mathbf{c}(y_0)$ to the estimated signature values. Note that in the probabilistic formulation in (3), the problem then reduces to estimating the prior distribution $p(y_0)$ and the distribution of the mismatch conditioned on the location, $p(\mathbf{z} \,|\, y_0)$. In the case of the mismatch due to i.i.d. zero-mean Gaussian additive error with variance σ^2, the PME with the knowledge of the correct variance σ^2 and the correct prior distribution $p(y_0)$ gives the best possible estimate in terms of mean square error, and equivalently, root mean square error (RMSE). Equation (3) rewritten for the observed difference between the estimated and the measured signal signature $\mathbf{z}$ in this case reads

$$\hat{y}_0(\mathbf{z}) = \sum_{y_0 \in \mathbb{D}} y_0 \frac{\exp(-\|\mathbf{z}\|_2^2 / 2\sigma^2)\, p(y_0)}{\sum_{y \in \mathbb{D}} \exp(-\|\mathbf{z}\|_2^2 / 2\sigma^2)\, p(y)}. \qquad (4)$$

5.2. LocUNet

Our recently presented LocUNet [12, 13, 14] takes pathloss radio map estimations and the measured RSS values from a set of N transmitters and returns a location estimation, see. Fig. 3 for a visualized summary of it. The first part of LocUNet is a UNet variant [24], returning a heatmap/a-posteriori distribution, followed by a final regression layer of center of mass operation that gives location estimates in terms of the coordinates. Its state-of-the-art performance in several settings with respect to RSS and ToA ranging-based methods were shown through numerical simulations for realistic urban scenarios and its code was set publicly available [1].

[1] https://GitHub.com/CagkanYapar/LocUNet

Table 1: Comparison of the accuracies of LocUNet and the probabilistic method in a Gaussian additive noise scenario.

Test metric:	**MAE**	**RMSE**	**MAE**	**RMSE**
# Tx:	3 Tx		5 Tx	
PME	20.91	30.11	10.55	16.43
LocUNet	21.17	30.41	11.28	17.63

In Table 1, we present the localization results of LocUNet and the presented probabilistic method, where we considered a scenario of presence Gaussian additive noise in RSS measurements, and where a UE is always located inside the 164×164 middle window measuring positive RSS from a random set of $N = 3, 5$ Tx. Assuming a (postulated, mismatched) prior of uniform distribution over all locations inside the 164×164 centered window that has positive RSS values on at least N out of the 80 available Tx for a city map, the probabilistic method is employed by using (4). The variance of the Gaussian noise was chosen as $\sigma^2 = 6.4$ dB^2. Note that LocUNet is oblivious to any prior information, yet it demonstrates very close performance.

5.3. ToA Ranging-Based Methods

In our LocUNet paper [13], we have provided comparisons with state-of-the-art ToA ranging-based algorithms using the *RadioToASeer Dataset*. The implementation of these methods were also set publicly available in the GitHub repository [1].

6. SHORT DESCRIPTION OF LOCSWINUNET

The only method that took part in the competition was *LocSwinUNet* [25], which is an adaptation of Swin transformer-based [26] SwinUnet [27] to the localization task. More specifically, a SwinUnet is extended by a final trainable regression layer that returns location coordinate estimates. Similar to LocUNet, *LocSwinUNet* can use both pathloss and ToA radio maps due to its ability to take different numbers of input image features. The results are shown in Table 2.

7. CHALLENGE RESULTS

The authors of the submitted method considered three different scenarios, which we describe below. Numerical experiments were performed considering different input features, namely pathloss and ToA radio maps, and city maps.

Scenario 1 (clean measurements, noisy radio maps): The pathloss radio maps are made noisy by adding a Gaussian noise $\sim \mathcal{N}(0, \sigma_p^2)$ with $\sigma_p = 10$ dB. Similarly, the ToA are also contaminated by am additive Gaussian noise $\sim \mathcal{N}(0, \sigma_t^2)$ with $\sigma_t = 20$ m. The Rx/Tx association setting provided in *RadioLocSeer* [13] was adopted. **Scenario 2 (clean measurements, noisy radio maps, new test set):** The trained model in Scenario 1 is evaluated on the evaluation dataset *LocRSSToATest* with a different Rx/Tx association setting than before. **Scenario 3 (noisy measurements, noisy radio maps, new test set):** This scenario represents the more realistic case of the presence of inaccuracies in the RSS and ToA measurements (cf. Sec. 3). The deviations of RSS and ToA measurements are modelled by additive zero-mean Gaussian noise terms, with standard deviations of $\sigma_p = 10$ dB and $\sigma_t = 10$ m. *LocSwinUNet* was trained over such noisy training dataset and then evaluated on the new test dataset *LocRSSToATest.* Due to time constraints of the competition, not all input feature combinations could be examined.

Table 2: RMSE performance of the submitted method [25].

Scenario	**RSS+ToA+City**	**RSS+ToA**	**RSS**	**ToA**
#1	2.048	**1.925**	5.896	2.879
#2	4.398	**3.361**	8.148	4.296
#3	10.14	N/A	N/A	N/A

8. CONCLUSIONS AND DISCUSSIONS

The results show the importance of using both pathloss and ToA radio maps and measurements as input features of the proposed neural network. Unfortunately, due to the time constraints of the competition, the authors were not able to provide comparisons with baselines, making it difficult to assess the performance of the proposed method relative to the state-of-the-art. We hope that this will be addressed in future work.

9. REFERENCES

[1] G. Bresson, Z. Alsayed, L. Yu, and S. Glaser, "Simultaneous localization and mapping: A survey of current trends in autonomous driving," *IEEE Transactions on Intelligent Vehicles*, vol. 2, no. 3, pp. 194–220, 2017.

[2] E. Pournaras, "Proof of witness presence: Blockchain consensus for augmented democracy in smart cities," *Journal of Parallel and Distributed Computing*, vol. 145, pp. 160–175, 2020.

[3] R. Di Taranto, S. Muppirisetty, R. Raulefs, D. Slock, T. Svensson, and H. Wymeersch, "Location-aware communications for 5G networks: How location information can improve scalability, latency, and robustness of 5G," *IEEE Signal Processing Magazine*, vol. 31, no. 6, pp. 102–112, 2014.

[4] J. Warrior, E. McHenry, and K. McGee, "They know where you are [location detection]," *IEEE Spectrum*, vol. 40, no. 7, pp. 20–25, 2003.

[5] S. Severi, H. Wymeersch, J. Härri, M. Ulmschneider, B. Denis, and M. Bartels, "Beyond GNSS: Highly accurate localization for cooperative-intelligent transport systems," in *IEEE Wireless Comm. and Networking Conf. (WCNC)*, 2018, pp. 1–6.

[6] A. Amini, R. M. Vaghefi, J. M. de la Garza, and R. M. Buehrer, "Improving GPS-based vehicle positioning for intelligent transportation systems," in *IEEE Intelligent Vehicles Symposium Proceedings*, 2014, pp. 1023–1029.

[7] I. Guvenc and C. Chong, "A survey on TOA based wireless localization and NLOS mitigation techniques," *IEEE Communications Surveys Tutorials*, vol. 11, no. 3, pp. 107–124, 2009.

[8] R. M. Vaghefi and R. M. Buehrer, "Received signal strength-based sensor localization in spatially correlated shadowing," in *2013 IEEE International Conference on Acoustics, Speech and Signal Processing*, 2013, pp. 4076–4080.

[9] P. Bahl and V. N. Padmanabhan, "RADAR: An in-building RF-based user location and tracking system," in *Proceedings IEEE INFOCOM 2000. Conference on Computer Communications.*, vol. 2, 2000, pp. 775–784.

[10] R. Levie, C. Yapar, G. Kutyniok, and G. Caire, "RadioUNet: Fast radio map estimation with convolutional neural networks," *IEEE Transactions on Wireless Communications*, vol. 20, no. 6, pp. 4001–4015, 2021.

[11] Ç. Yapar, R. Levie, G. Kutyniok, and G. Caire, "Real-time localization using radio maps," *arXiv preprint:2006.05397*, 2020. [Online]. Available: https://arxiv.org/abs/2006.05397

[12] ——, "LocUNet: Fast urban positioning using radio maps and deep learning," in *ICASSP 2022 - 2022 IEEE International Conference on Acoustics, Speech and Signal Processing (ICASSP)*, 2022, pp. 4063–4067.

[13] ——, "Real-time outdoor localization using radio maps: A deep learning approach," *IEEE Transactions on Wireless Communications*, 2023.

[14] Ç. Yapar, F. Jaensch, R. Levie, G. Kutyniok, and G. Caire, "On the effective usage of priors in rss-based localization," *arXiv preprint:2212.00728*, 2022. [Online]. Available: https://arxiv.org/abs/2212.00728

[15] Ç. Yapar, R. Levie, G. Kutyniok, and G. Caire, "Dataset of pathloss and ToA radio maps with localization application," 2022. [Online]. Available: https://dx.doi.org/10.21227/0gtx-6v30

[16] ——, "Dataset of pathloss and ToA radio maps with localization application," *arXiv preprint:2212.11777*, 2022. [Online]. Available: https://arxiv.org/abs/2212.11777

[17] OpenStreetMap contributors, "Planet dump retrieved from https://planet.osm.org ," https://www.openstreetmap.org, 2017.

[18] R. Hoppe, G. Wölfle, and U. Jakobus, "Wave propagation and radio network planning software WinProp added to the electromagnetic solver package FEKO," in *Proc. Int. Appl. Computational Electromagnetics Society Symp. - Italy (ACES)*, Florence, Italy, March 2017.

[19] R. Hoppe, G. Wölfle, and F. Landstorfer, "Fast 3-D ray tracing for the planning of microcells by intelligent preprocessing of the data base," in *3rd European Personal and Mobile Communications Conference (EPMCC)*, 1999.

[20] G. Wölfle, R. Hoppe, and F. M. Landstorfer, "A fast and enhanced ray optical propagation model for indoor and urban scenarios, based on an intelligent preprocessing of the database." Citeseer.

[21] R. Wahl, G. Wölfle, P. Wertz, P. Wildbolz, and F. Landstorfer, "Dominant path prediction model for urban scenarios," in *14th IST Mobile and Wireless Communications Summit*, 2005.

[22] I. Stepanov and K. Rothermel, "On the impact of a more realistic physical layer on MANET simulations results," *Ad Hoc Networks*, vol. 6, no. 1, pp. 61–78, 2008.

[23] F. Pérez-Cruz, P. M. Olmos, M. M. Zhang, and H. Huang, "Probabilistic time of arrival localization," *IEEE Signal Processing Letters*, vol. 26, no. 11, pp. 1683–1687, 2019.

[24] O. Ronneberger, O. Fischer, and T. Brox, "U-Net: Convolutional networks for biomedical image segmentation," in *Medical Image Computing and Computer-Assisted Intervention – MICCAI*, N. Navab, J. Hornegger, W. M. Wells, and A. F. Frangi, Eds. Cham: Springer International Publishing, 2015, pp. 234–241.

[25] M. Hu, S. Xu, Q. Liu, M. Katwe, C. Yuen, and S. G. Razul, "LocSwinUNet: A neural network for urban wireless localization using ToA and RSS radio maps," in *2023 IEEE 33nd International Workshop on Machine Learning for Signal Processing (MLSP)*, 2023.

[26] Z. Liu, Y. Lin, Y. Cao, H. Hu, Y. Wei, Z. Zhang, S. Lin, and B. Guo, "Swin transformer: Hierarchical vision transformer using shifted windows," in *Proceedings of the IEEE/CVF International Conference on Computer Vision (ICCV)*, October 2021, pp. 10 012–10 022.

[27] H. Cao, Y. Wang, J. Chen, D. Jiang, X. Zhang, Q. Tian, and M. Wang, "Swin-Unet: Unet-like pure transformer for medical image segmentation," in *Computer Vision – ECCV 2022 Workshops*, L. Karlinsky, T. Michaeli, and K. Nishino, Eds. Cham: Springer Nature Switzerland, 2023, pp. 205–218.